“CBDynamics”: Approaches to the Synthetic Production of Cannabidiol for Medicinal Purposes.

Team leaders: Padula, B.R.; Redígolo, J.L.S.
Team members: Andraus. M.Q.; Araujo, G.N.; Carneiro, A.G.; Batalha, E.H.P.S.; Katsumata, L.M.; Kiura, G.T.; Oliveira, M.B.; Tavares, S.C.; Silva, M.B.; Silva, L.A.R.
PIs: Moreni, André L.; Segato, Fernando* **Advisor:** dos Santos, Júlio César
*e-mail: symb-lab@usp.br

ARTICLE INFO

Keywords:
Canabidiol
Cannabis sativa
Olivetolic acid
Therapeutic
Chronic diseases

ABSTRACT

Cannabidiol (CBD) is a valuable medical compound known for its numerous therapeutic benefits, particularly in the treatment of patients with chronic diseases, such as epilepsy. However, in Brazil, its acquisition is shrouded in bureaucratic and legal complexities, primarily stemming from its association with *Cannabis sativa*. Therefore, this study aims to produce cannabidiolic acid (CBDA), the direct precursor to CBD, using biosynthesis and recombinant gene technology with *Saccharomyces cerevisiae*. This process involves two essential pathways: the geranyl diphosphate (GPP) pathway, already present in the native yeast metabolism, and the olivetolic acid pathway, native to *C. sativa*. Consequently, both precursors will be combined in a second reaction to form cannabigerolic acid, which will then be converted into cannabidiolic acid, which can be purified and converted into CBD, as well as an optimization proposal that encompassed a kinetic study,recombinant gene technology and bioreactor studies. Finally, this innovative alternative method seeks to provide a more affordable and less bureaucratic way for patients to obtain CBD, thereby significantly enhancing patient access to this valuable therapeutic compound.

1. INTRODUCTION

The pursuit of less aggressive therapies using compounds of natural origin has grown significantly in recent decades, particularly for the treatment of various neurological conditions such as autism spectrum disorder, Parkinson's disease, and epilepsy (NUNES, 2021). In this context, the *Cannabis sativa* plant, which has been widely used for its medicinal properties by civilizations such as those of China and India for centuries, shows great promise in treating these conditions. This potential is largely attributed to one of its neurologically active components, cannabidiol (CBD).

Although CBD is already utilized in pharmaceutical formulations, its use faces government restrictions in many countries due to the controlled nature of the *C. sativa* cultivation and use. This is primarily because the plant is known for its psychoactive effects, which result from the combined action of its numerous psychoactive compounds (NIDA, 2024). The Brazil Law No. 11.343/2006, known as “the Drug Law”, prohibits the cultivation of *Cannabis sativa* due to concerns about its abusive misuse. However, after a lengthy democratic process, the use of cannabidiol for treating several clinical conditions is now allowed when recommended and prescribed by a licensed medical doctor, provided all necessary health regulations are met (Law No. 17,618/23).

Despite this progress, access to these medications remains challenging. It is well-documented that the process of acquiring CBD-based products is not only bureaucratic but also prohibitively expensive, making these treatments inaccessible to many patients.

In light of the numerous obstacles patients face when seeking for cannabidiol therapies, a promising scientific alternative has emerged: the production of CBD through synthetic routes. This is the goal of the CBDynamics project, which aims to

produce cannabidiol using yeasts. This innovative approach seeks to overcome the barriers associated with *Cannabis sativa* cultivation and provide its powerful active ingredient for the development of novel medications, ultimately benefiting patients in need.

2. MATERIALS AND METHODS

2.1. Optimization Cassetes

In this team's previous work (https://2023.igem.wiki/usp-eel-brazil/), biological circuits for the biosynthesis of cannabidiolic acid (CBDA), the precursor molecule to CBD, using *Saccharomyces cerevisiae* as a chassis were developed. The pathways cassettes for olivetolic acid and CBDA production were planned for cloning in appropriate shuttle plasmids. To simplify genetic manipulations and optimize substrate conversion, the genes were divided into two circuits. Inserts were designed with intercalated T2A sequences to maintain protein functionality and enable the effective expression of multiple proteins from a single mRNA. The circuits were designed for cloning into pRS423 and pRS426 vectors using Gibson Assembly, under the regulation of the *Gal1* promoter and *ADH1* terminators, with appropriate selection markers. SnapGene Viewer was utilized to visualize and assemble the plasmids, and 72 plasmid variants were evaluated. After said evaluation, two adequate biological circuits were selected for further studies.

To enhance CBD production in yeast, this study focused on optimizing enzyme expression and substrate accumulation without heavily burdening the yeast strain's metabolism. The primary goal was to increase the accumulation of geranyl pyrophosphate (GPP), a key precursor in cannabinoid biosynthesis, by either reducing its conversion into secondary metabolites or promoting its overproduction. To achieve this, two main strategies were developed.

The first strategy involved RNA interference (RNAi) in order to partially suppress the activity of the *ERG20* enzyme, which converts GPP into farnesyl pyrophosphate (FPP). The goal was to attenuate *ERG20* activity, without completely silencing it, ensuring essential cellular processes remained functional. Furthermore, by controlling the RISC system expression via regulated promoters, the gene silencing could be activated in a timely fashion. iRNA silences genes by identifying hairpin dsRNA strands, which turns on the RISC system, consisting of the *DICER* and *Argonaute (ARG)* enzymes. The *Dicer* enzyme fragments the dsRNA hairpin into 10-20bp fragments, which are incorporated by the *ARG*. These incorporated fragments work as guides, promoting degradation of complementary RNAs by the *ARG* enzyme, effectively attenuating the translation stage (Chen, Guo, Zhang, & Si, 2020).

Since *S. cerevisiae* lacks the RISC system, additional cassettes were developed to integrate the system into *the S. cerevisiae* genome (Pratt & MacRae, 2009). The RNAi cassette used a tetracycline-inducible promoter (*pTet*) and recyclable selection marker (*URA3*), along with internal ribosome entry sites (*IRES*) to facilitate translation.

The design of the GPPS overexpression cassette focused on utilizing the *HXK2* promoter to drive high levels of *geranyl pyrophosphate synthase* (GPPS) expression, thereby increasing GPP availability for cannabinoid biosynthesis. Additionally, the cassette was engineered with homologous recombination sites and polylinker enzymes to enable future modifications, ensuring greater adaptability and flexibility in the biomanufacturing process. To further enhance GPP production, the *HXK2* gene was silenced, promoting the overexpression of *HXK1* and redirecting the glycolytic flux toward the mevalonate (MVA) pathway, which is critical for GPP synthesis (Sun et al., 2014).

All cassettes were designed with homology sites integrated into the 5'UTR and 3'UTR regions, enabling precise genome incorporation by homologous recombination. For RNAi, the *pep4* protease locus was identified as an ideal recombination and knockout target, as its deletion did not significantly affect yeast growth (Schoborg et al, 2016). Similarly, silencing HXK2 in the GPPS overexpression cassette redirected metabolic activity, improving enzyme function without hindering overall cellular mechanisms. These strategies collectively aim to optimize GPP availability and improve the efficiency of CBD production in the yeast chassis.

2.2. Kinetic Modelling

Another essential aspect of the project was optimizing enzymatic reactions for CBD production by determining the ideal concentration of hexanoic acid to be added during fermentation in order to maximize CBDA output while preserving enzyme

activity. Kinetic modeling and data analysis were employed to identify optimal conditions for enhancing CBD production.

To derive the kinetic velocity equations for the enzymes involved—Cannabidiolic Acid Synthase (CBDAS), Olivetolic Acid Cyclase (OAC), Prenyltransferase 4 (CsaPT4/PT4), Hexanoyl-CoA Synthase (CsHCS1), and Olivetol Synthase (OLS)—data was gathered from the Brenda Enzyme and KEGG databases (Kanehisa & Goto, 2000; Chang et al., 2021).

To analyze the kinetic profiles of these enzymes, the Michaelis-Menten model was applied. This model is a cornerstone of biochemistry, describing how the rate of an enzyme-catalyzed reaction depends on substrate concentration (Leow & Chan, 2019). The Michaelis-menten model was chosen due to its prominence in enzyme kinetics studies, and due to it being a mass-action kinetic model, which explains in high-fidelity the interactions between enzymes. This modeling was performed in an "isolated" system, excluding considerations of background influences, competition, and other intracellular factors inherent to the cellular environment (Bauermann et al., 2022).

Two critical constants were determined for each enzyme: the maximum reaction rate (Vmax) and the Michaelis constant (Km). For CBDAS, these values, along with substrate concentration, were effectively obtained from the UniProt, BRENDA databases and the study by Wiles et al. (2022), as its behavior aligns with the Michaelis-Menten model (UniProt Consortium, 2025).

Although a Km value for the enzyme Prenyltransferase 4 (CsaPT4) was available in the literature, no corresponding Vmax value was reported (Fellermeier & Zenk, 1998). To resolve this, a BLAST alignment was conducted using the NCBI database. This analysis identified 14 enzymes with at least 40% similarity to CsaPT4 that had reported Km values and were not specific to *Cannabis sativa*.

The enzymes selected for this analysis included homologs such as *Humulus lupulus 2-acylphloroglucinol 4-prenyltransferase*, aromatic prenyltransferase isolates, and homogentisate solanesyltransferase (*HST1*) from *Aquilaria malaccensis*. Additionally, various proteins from *Pelargonium* species and *Arabidopsis thaliana* homogentisate homogentisate phytyltransferase *VTE2-2* were included.

Using the T-Coffee MUSCLE package, a phylogenetic analysis was conducted with ClustalW alignment, ensuring 90% conservation (Notredame, Higgins, & Heringa, 2000; Madeira et al., 2024). In this analysis, we compared the catalytic site alignments of these enzymes with CsaPT4 to identify conserved regions.

Figure 1: CsaPT4 phylogenetic analysis

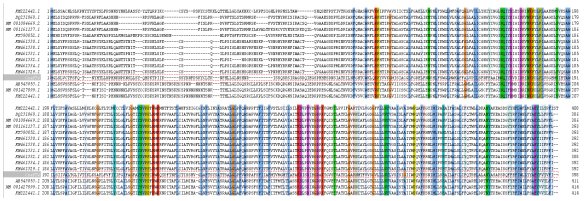

A phylogenetic tree was constructed to evaluate the proximity of the selected enzymes with *CsaPT4*. Based on the similarity values, the mean and standard deviation of the Km and Vmax values were calculated to estimate these parameters for CsaPT4.

Figure 2: CsaPT4 phylogenetic tree

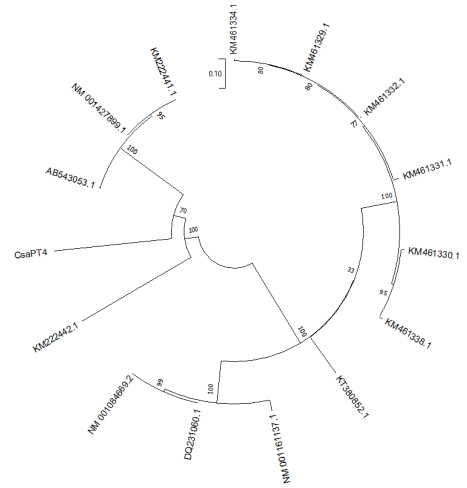

No Km or Vmax values for olivetolic acid cyclase (*OAC*) were found in the literature or reference databases. Attempts to use a method similar to that for *CsaPT4* faced challenges to a lack of enzymes with sufficient similarity to *OAC* and available kinetic data.

OLS, *CBDAS*, and *CsaPT4* exhibited Km and turnover number (Kcat) values derived from the UniProt database and Wiles et al. (2022). This

constant directly relates to Vmax providing insights into maximum reaction rates.

For Hexanoyl-CoA Synthase (*CsHCS1*), Km and Vmax values for hexanoic acid were obtained from the UniProt database. *CsHCS1* follows a kinetic model that includes substrate inhibition, described by a modified Michaelis-Menten equation. It was observed that high CoA concentrations caused inhibitory effects, which were accurately modeled using this modified equation (Stout et al., 2012).

2.3. Bioreactor

The objective of utilizing a bioreactor in CBDynamics is to model a scale-up in CBD production, whilst optimizing this production in regards to biomass accumulation, growth stage and substrate uptake. As described by Borowiak et al. (2012), the methodology aims to maximize yeast growth while preventing diversion toward ethanol production. Ethanol production reduces total biomass yield, either due to oxygen limitation in the medium or the microorganism's positive Crabtree effect (Belo; Pinheiro; Mota et al., 2003).

The transformed yeast is designed to produce CBDA during its stationary growth phase without compromising overall growth or final yield. The growth curve for our particular strain needed to be developed, as there were none available from previous studies.

To achieve optimal growth and CBD production, the bioreactor conditions were tailored to the specific requirements of the proposed yeast strain. Higher biomass yields can be achieved by controlling nutrient supply to the reactor, as suggested by Borowiak et al. (2012). The nutrients' medium supply over time can be modeled using the logistic equation (1), with a (g), b and c (h^{-1}) as its parameters.

$$g(t) = \frac{a}{(1+be^{-ct})} \quad (1)$$

To further refine the model, the parameters of Equation (1) were adjusted to optimize the inflow of the nutrient medium. This was achieved by deriving a formula that maximized the criterion K, where K = Yμ. In this expression, Y represents the biomass yield, and μ is the specific growth rate. The parameters of this modified model were influenced by the initial biomass concentration, as outlined by Borowiak et al. (2012).

The model was validated by extending the initial data from Equation (1) to the yeast strain under study. By maintaining experimental conditions similar to those described by Borowiak et al., the consistency of these initial estimates could be tested.

For that to be done, the authors' optimized parameters were taken in the concentration that seemed appropriate to the bioreactor available in order to determine the nutrient medium supply time and volume using the following equation:

$$t_{on} = \frac{g(t+\Delta t)-g(t)}{G_c W} \quad (2)$$

In (2); g(t): glucose medium supply term as a function; G_c: glucose concentration in the nutrient medium (g/L) and W: rate of delivery of the nutrient-dosing peristaltic pump (0,96 L/h).

The medium was fed in batches every 30 minutes, and samples were collected at one-hour intervals, with 2 mL per sample. Borowiak's model was applied, as it accurately represents the glucose supply profile during S. cerevisiae growth. Dissolved oxygen tension, measured as a percentage of saturation, served as a control parameter. Environmental factors such as aeration, pH, and temperature were kept constant throughout the experiment to ensure consistency. The logistic equation was also employed to determine the ideal glucose concentration as a function of time, based on experimental parameters. Dissolved oxygen levels were carefully monitored, as they play a critical role in aerobic processes. Excessively high oxygen levels indicated reduced cellular oxygen consumption, potentially signaling the onset of the death phase. To ensure accurate growth modeling, the logistic equation was applied to establish the ideal glucose concentration profile over time.The introduction of the inducers (galactose and tetracycline) will take place in the stationary phase to start the production of CBDA without impacting cell growth.

2.4. Wet-lab

2.4.1. pRS423 construction

The *pSB1A3-ScHIS3* plasmid, carrying the *ScHIS3* selection marker, available from the *iGEM23 distribution kit,* was transformed into *E. coli* competent cells by heat shock. Colonies carrying the plasmid after transformation were identified by colony PCR Positive colonies were inoculated into

LB-Amp and incubated overnight. Plasmids were purified from the overnight culture using Cytiva's PlasmidPrep kit and used as template DNA for amplifying the *ScHIS3* marker with homology overhangs for cloning by the Gibson Assembly method.

The *pRS426* plasmid was purified from an *E. coli* stock carrying the plasmid, as described before. Both the *ScHIS3 marker* and pRS426 were amplified by PCR, and the purified the fragments were fused with the Gibson Assembly method. For the reaction 0,5µL of the purified *ScHIS3* fragment, 4,5µL of the purified pRS backbone and 15µL of Gibson Assembly Master Mix were mixed. he reaction was set up on ice and incubated at 50ºC for 40 minutes. After the incubation time, this reaction was transformed into competent *E. coli* cells by heat shock.The transformed cells were plated on LB-Amp plates, incubated overnight, at 37ºC. Visible colonies were tested by colony PCR, and positive colonies were inoculated into fresh LB-Amp media and incubated overnight. Following incubation, plasmid purification proceeded as described before. This new construct was termed *pRS423s*, due to the substitution of the URA3 selection marker for the *HIS3* selection marker.

2.4.2. ***CBDsub* and *CBDsyn* Cassettes**

Synthetic DNA fragments obtained from IDT DNA were resuspended in TE buffer, as instructed by the manufacturer and used as templates for amplification by PCR, using primers designed to add homology regions for fragment fusion and cloning into the *pRS* plasmids by Gibson Assembly. The *pRS426* and *pRS423s* plasmids were also amplified by PCR, including complementary regions to the amplified gene fragments.

The amplified and purified fragments were cloned into the linearized plasmids by Gibson Assembly, followed by *E. coli* transformation by heat shock and colony PCR. Positive colonies were cultured, miniprepped, and digested with *KpnI*. Correct digestion patterns confirmed successful cloning of the *CBDsub* cassette into *pRS426* and *CBDsyn* into *pRS423s*.

2.4.3. ***Yeast transformation***

50 µL of *Saccharomyces cerevisiae*, stored at -70°C and streaked onto solid YPD-9721 were agarsing a flamed platinum loop and incubated at 30ºC for 48 hours. A small amount of yeast was collected using a sterile loop and inoculated into medium in an Erlenmeyer flask. The culture was incubated at 30°C with shaking at 180 rpm for 18 hours to promote cell growth. Subsequently, about four rounds of subculturing were conducted every two days to reactivate the yeast strain following extended storage at ultra-low temperatures.

To ensure a robust and viable culture, the yeast was replated on solid medium. Competent cell preparation was then initiated. An isolated colony of the SC9721 strain was transferred to an Erlenmeyer flask containing 10 mL of YPD medium, comprising 2.0% peptone, 1.0% yeast extract, and 2.0% glucose. The culture was incubated at 30°C under shaking at 200 rpm for 16 hours.

After incubation, 5 mL of the culture was inoculated into a fresh YPD medium and incubated under identical conditions for an additional 4 hours. The cells were centrifuged at 5,000×g for 5 minutes, followed by washing the pellet with 20 mL of sterile MilliQ water and another round of centrifugation. The final preparation involved resuspending the cells in 1 mL of TE/LiAc solution.

For transformation reactions, 100 µL of the competent cell suspension was used per reaction. The cell suspension was divided into Falcon tubes, centrifuged at 16,000×g for 20 minutes, and the supernatant was discarded. The pellet was resuspended in saline solution, and the competent cell stocks were stored in refrigeration.

Unfortunately, due to time constraints, we were unable to complete the transformation experiments before the end of the academic year at our institution. As a result, we were unable to finalize the experiments within the planned timeframe, which has delayed our ability to draw conclusive results and move forward with the next steps of the project. We remain committed to continuing this work in the upcoming academic year and anticipate completing the experiments as soon as possible.

3. RESULTS AND DISCUSSION

3.1. Optimization Cassetes

To enhance the understanding and facilitate the design process, the cassettes were, initially, constructed as linear fragments. This approach provided a clear and concise visual representation of

the entire cassette, aiding in the assessment of size and overall structure. Moreover, the linear assembly allowed us to easily track the progressive addition of components, providing valuable insights and facilitating learning throughout the construction process.

The research and subsequent planning outlined a novel approach to enhance GPP production in yeast cells through a combination of RNA interference (RNAi), based on the planning for introduction of the RISC system into the yeast cells' genome, in order to selectively downregulate the expression of *ERG20*, and *GPPS* overexpression. The constructed cassettes can be seen in Figure 3, as visualized on SnapGene.

This work highlights the power of synthetic biology to engineer yeast for enhanced secondary metabolite production. The final results suggest that by carefully designing and optimizing biological circuits, the increase of GPP levels, a critical precursor for CBD biosynthesis, can theoretically be achieved and analyzed through GEMs, or genome-scale metabolic models, which are comprehensive mathematical representations of an organism's metabolic network. These models simulate chemical reactions within the cell and allow the prediction of the impact of genetic and environmental changes on cellular behavior. In this context, GEMs can be instrumental in optimizing yeast strains for enhanced CBDA synthesis. By simulating the introduction of exogenous biological circuits into yeast cells, we can predict and analyze the potential impact on CBDA production efficiency, guiding the development of more robust and effective strategies. These results provide a strong foundation for future research aimed at developing efficient and sustainable methods for producing plant-derived cannabinoids.

3.2. Kinetic Modeling

The mean and standard deviation of the Km and Vmax values of enzymes similar to CsaPT4 were used as estimates for the enzyme's actual values, corresponding to 5.7 µM and 0.1 µmol/g/min, respectively. As previously described, although the same procedure was applied to the enzyme OAC, it was not possible to obtain Km and Vmax values for similar enzymes to perform statistical analyses.

In this context, research indicates that OAC is a polyketide cyclase that catalyzes the C2-C7 aldol cyclization of linear pentyl tetra-β-ketide CoA, resulting in the formation of olivetolic acid (OA) (Yang et al., 2016; Gagne et al., 2012).

OLS facilitates the conversion of hexanoyl-CoA and malonyl-CoA into olivetol, which is subsequently transformed into OA by OAC. The kinetic behavior of both enzymes can be effectively described through the kinetics of OLS, as it represents the rate-limiting step in the reaction pathway. Consequently, the initial velocity of OAC is not calculated, as the overall process efficiency is predominantly determined by OLS activity.

By utilizing the ratio of the maximum kinetic velocity to the mass of substrate used, it is possible to determine the relative kinetic velocity corresponding to the amount of substrate employed. Additionally, to calculate the Vmax of OLS based on the Kcat kinetic parameter reported in the literature, the relationship between these parameters and the enzyme

Figure 3: Biological circuits: (A) pUC57:RISC, (B) pUC57:RNAi for silencing and (B) pRS426 for superexpression.

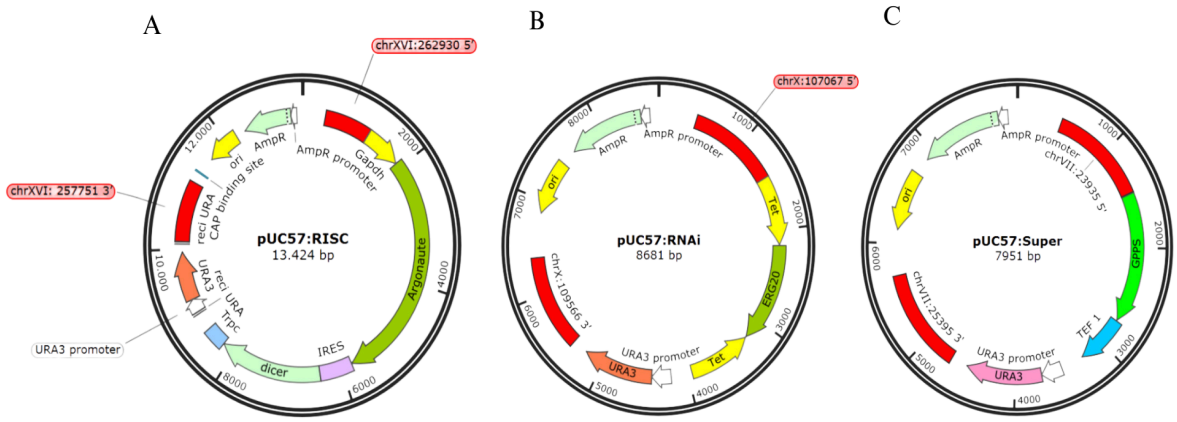

concentration was utilized. This calculation employed the formula Vmax = [E] \ Kcat, where [E] represents the enzyme concentration. Using the Km and Vmax values for each enzyme, kinetic velocity profile graphs were plotted, and the initial reaction rate was calculated employing the Michaelis-Menten kinetic equation (Wiles et al., 2022). For the enzyme CsHCS1, the calculation incorporated the modified Michaelis-Menten equation that accounts for substrate inhibition (Stout et al., 2022). The Km, Vmax, and V_0 values for each enzyme are presented in the table below.

Table 1: Enzymes kinetics parameters

	Km	Vmax	Vo
CBDAS	0.137 mM	2.57 nmol/s/mg	1.006 pKat
CsaPT4	5.7 µM	0.1 µmol/g/min	1.62 nmol/g/s
OLS	60.8 µM	5.792 nmol/L.s	4.442 nmol/L.s
CsHCS1	3.7 mM	0.68 aKat	0.643 amol/s

Figure 4: CBDAS, CsaPT4, OLS and CsHCS1 enzyme kinetic velocity profile graph, respectively.

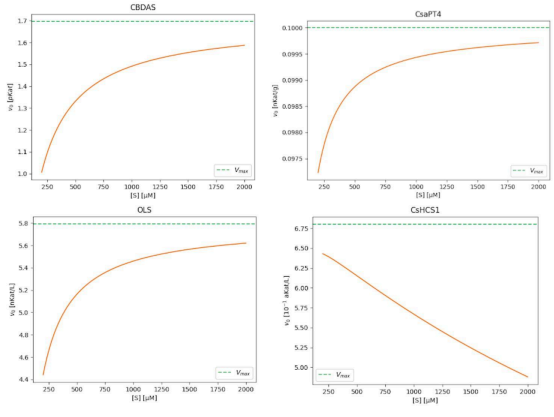

In the kinetic profile for the *CsHCS1* enzyme, the units were adjusted to aKat (10^{-18})to facilitate data interpretation. The theoretical concentration of hexanoic acid, the substrate supplied to the cells, was calculated to be approximately 200 µM. This value was determined by performing the stoichiometry of each reaction in which the enzymes listed above are involved in CBD production. Several assumptions were made during this process: all other reagents were maintained in excess, and the conversion of reagents to products occurred without significant losses. This theoretical value provides a foundation for wet laboratory testing, enabling a more efficient screening of fermentation parameters to maximize CBDA production.

3.3. Bioreactor

When analysing the results obtained from the bioreactor experiment, the analysis of the carbon source utilized - in this case, glucose - throughout the process is essential. In figure 5, it is displayed an ideal glucose mass of 0,1 g/L. This is done in order to prevent the yeast's metabolism to divert itself to ethanol production through the Crabtree effect. A curve showing the fed glucose into the reactor is also shown, calculated using the volume of medium inoculated into it every 30 minutes. It shows a gradual increase, as the calculation was made to add more glucose as the inoculated cells consumed it. Finally, it is shown the remaining glucose in the medium, which wasn't consumed. Analyzing the entirety of data, it is clear that the initial concentration of cells added to the reactor was not enough to consume all the glucose fed - otherwise, the remaining glucose would have similar values to the ideal. This demonstrated the need to increase the initial concentration of cells to be inoculated into the reactor, so that glucose is nearly fully consumed prior to the next feeding. Another proposition is reducing the glucose feeding concentration, or extending the time between feeds. This unexpected result comes from the strain's growth kinetics variations, which exceeded expectations.

Figure 5: Comparison between fed, remaining and ideal glucose in medium.

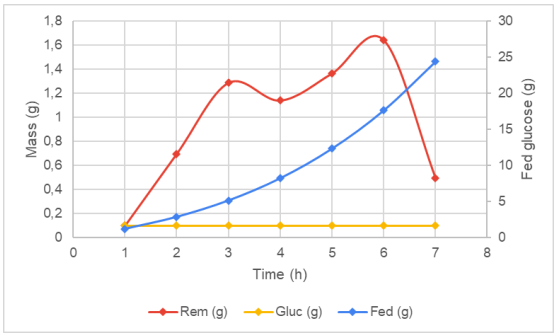

When analyzing cell mass and glucose mass, however, Figure 6 shows that the cell mass curve obtained in this experiment is similar to an ideal microbial growth curve. This is shown by the phases

it displays: lag, exponential and stationary. Therefore, the model proposed by Borowiak et al, 2012 can be used to predict the cell mass of the selected yeast strain as the fermentation progresses, giving insights to the exact moment the induction of gene expression should be initiated.

It is also clear that the results obtained are reasonable - when comparing the aforementioned glucose mass curve against the cell mass curve in Figure 6, it is evident that as the biomass increased, the medium carbon source decreased proportionally.

Figure 6: Comparison between consumed glucose and cell mass during the experiments

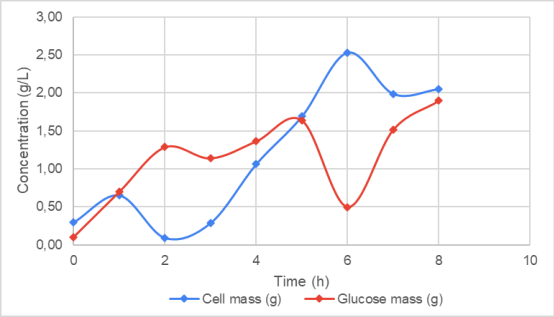

It is finally concluded that understanding the balance between nutrient availability and cell growth is key, particularly when planning the ideal moment to trigger CBDA production in the engineered yeast without negatively impacting either bioproduct or biomass yields. The proportional relationship between cell mass increase and glucose consumption observed in the experiment supports the reliability of this team's findings and strengthens their relevance for optimizing biotechnological workflows.

3.4. Wet-lab

The construction and cloning experiments yielded successful outcomes, encompassing the assembly of the pRS423 plasmid and the cloning of genetic cassettes. The assembly of pRS423 was achieved using Gibson Assembly and subsequently verified through colony PCR and enzymatic digestion, confirming the replacement of the URA3 marker with the ScHIS3 marker. Amplification of the requisite genetic fragments, including the ScHIS3 marker and the pRS426 plasmid backbone, produced amplicons of expected sizes, as demonstrated by agarose gel electrophoresis. These results attest to the specificity of the primers and the efficacy of the purification procedures employed.

The successful cloning of genetic cassettes was also corroborated through PCR and visualization on agarose gels. Specifically, the CBD-sub cassette was integrated into the pRS426 plasmid, while the CBD-syn cassette was incorporated into pRS423. The accuracy of these integrations was confirmed by colony PCR, as illustrated in the figures below:

Figure 7: Colony PCR of pRS426-CBD-sub visualized on an agarose gel.

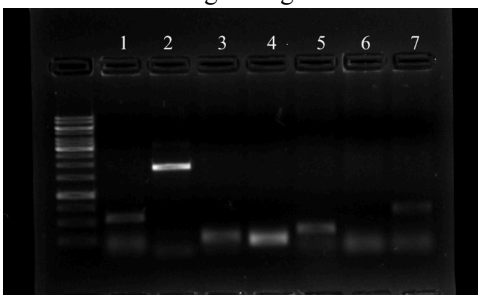

Figure 8: Colony PCR of pRS423s-CBD-syn visualized on an agarose gel.

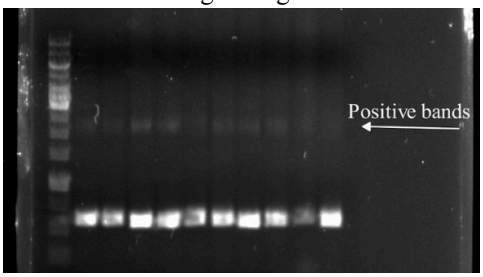

Bacterial transformation conducted to amplify the constructed plasmids demonstrated high efficiency, yielding viable colonies containing the correctly assembled plasmids. These findings were substantiated by subsequent molecular analyses.

Nevertheless, the transformation of Saccharomyces cerevisiae with the pRS423 plasmid has not yet been finalized due to the requirement for refinements in the standard lithium acetate transformation protocol. Specific optimizations under consideration include adjustments to incubation conditions and the composition of transformation mixtures to enhance the efficiency and stability of plasmid integration within the yeast chassis. These results represent significant progress and establish a robust foundation for the continuation of experimental procedures, with a primary focus on the functional validation of the constructed genetic systems.

4. HUMAN CENTERED DESIGN

In order to achieve an impactful project and reach a wider audience, the project's human-centered design focused on analyzing and consulting stakeholders and organizing events that promote diversity and inclusivity in science. The team was aided by various sectors of society, including patient associations and legal representatives, whose feedback improved and refined the overall scope of the project. Moreover, the inclusivity-focused events were planned to engage with certain groups, by the invention of props and adaptations, primarily centered around different age ranges, such as children and the elderly, and people with reduced mobility or visibility. This human-centered approach has the potential to significantly impact various sectors of society.

Academic research validates its scientific feasibility, paving the way for advancements in therapeutic applications. By actively engaging with public organizations, the local community, and government stakeholders, the project ensures that its development aligns with societal needs and regulatory frameworks. This collaborative approach fosters a deeper understanding of patient needs and allows for the development of more accessible and affordable CBD-based treatments, potentially revolutionizing the CBD industry and improving overall public health.

This project, aligned with the human-centered approach highlighted earlier, emphasizes the importance of collaborating with various stakeholders to advance CBD-based treatments and expand their societal impact. It integrates the scientific community, therapeutic sectors, biotechnology, and synthetic biology to drive research and develop innovative solutions, while also working with public organizations, such as the Unified Health System (SUS), to facilitate access to medications. Through inclusive events targeting diverse age groups and conditions, the project reinforces the importance of accessible and tailored initiatives.

Despite the potential of CBD for conditions such as ADHD, regulatory challenges and the need for more robust studies remain, underscoring the importance of a collaborative and innovation-driven approach focused on public health and inclusion. Furthermore, the team dedicated itself to sparking interest in science across different segments of society. Conducted interactive activities were led with groups of children in vulnerable social situations, highlighting how science is present in daily lives and can be fun. Young people and teenagers on the verge of entering university were also contemplated, showcasing the opportunities that science can offer and emphasizing that it is neither distant nor inaccessible to them.

Additionally, with a focus on inclusion, ways to make the laboratory environment more accessible were discussed, and equipment adapted for visually impaired individuals were developed. The positive feedback received after these projects was extremely rewarding, demonstrating the significant impact achieved.

5. CONCLUSION

Our team has directed its efforts into the development of an optimized, scalable, market-competitive synthetic production of cannabidiol (CBD), the bioproduct of interest. These efforts have allowed for the development of a theoretical precise manipulation of gene expression, facilitating the construction of metabolic pathways and innovative optimization routes for the production and accumulation of our bioproduct. In addition to the collaboration between the dry- and wet-lab experiments, it enabled a continuous cycle of improvements due to the modular nature of all designed parts, inline with the conceptualization of synthetic biology.

Furthermore, by consolidating the knowledge from multiple studies and providing a possible path for future investigations, this work serves as a valuable resource for investigators in the field of cannabinoid research and biotechnology.

6. REFERENCES

Bauermann, J., Laha, S., McCall, P. M., Jülicher, F., & Weber, C. A. (2022). Chemical kinetics and mass action in coexisting phases. Journal of the American Chemical Society, 144(42), 19294-19304. https://doi.org/10.1021/jacs.2c06265

Borowiak, D., Miśkiewicz, T., Miszczak, W., Cibis, E., & Krzywonos, M. (2012). A straightforward logistic method for feeding a fed-batch baker's yeast culture. *Biochemical Engineering Journal*, *60*, 36–43. https://doi.org/10.1016/j.bej.2011.09.016

Brand, E. J., & Zhao, Z. (2017). Cannabis in Chinese Medicine: Are Some Traditional Indications Referenced in Ancient Literature Related to Cannabinoids? *Frontiers*

in Pharmacology, *8*(108). https://doi.org/10.3389/fphar.2017.00108

Chang, A., Jeske, L., Ulbrich, S., Hofmann, J., Koblitz, J., Schomburg, I., ... & Schomburg, D. (2021). BRENDA, the ELIXIR core data resource in 2021: new developments and updates. Nucleic acids research, 49(D1), D498-D508. https://doi.org/10.1093/nar/gkaa1025

Chen, Y., Guo, E., Zhang, J., & Si, T. (2020). Advances in RNAi-Assisted Strain Engineering in Saccharomyces cerevisiae. *Frontiers in Bioengineering and Biotechnology*, *8*. https://doi.org/10.3389/fbioe.2020.00731

Fellermeier, M., & Zenk, M. H. (1998). Prenylation of olivetolate by a hemp transferase yields cannabigerolic acid, the precursor of tetrahydrocannabinol. FEBS letters, 427(2), 283-285. https://doi.org/10.1016/S0014-5793(98)00450-5

Gagne, S. J., Stout, J. M., Liu, E., Boubakir, Z., Clark, S. M., & Page, J. E. (2012). Identification of olivetolic acid cyclase from Cannabis sativa reveals a unique catalytic route to plant polyketides. *Proceedings of the National Academy of Sciences*, *109*(31), 12811–12816. https://doi.org/10.1073/pnas.1200330109

Kanehisa, M., & Goto, S. (2000). KEGG: kyoto encyclopedia of genes and genomes. Nucleic acids research, 28(1), 27-30. https://doi.org/10.1093/nar/28.1.27

Leow, J. W. H., & Chan, E. C. Y. (2019). Atypical Michaelis-Menten kinetics in cytochrome P450 enzymes: A focus on substrate inhibition. *Biochemical Pharmacology*, *169*, 113615. https://doi.org/10.1016/j.bcp.2019.08.017

Madeira, F., Madhusoodanan, N., Lee, J., Eusebi, A., Niewielska, A., Tivey, A. R., ... & Butcher, S. (2024). The EMBL-EBI Job Dispatcher sequence analysis tools framework in 2024. Nucleic Acids Research, gkae241. https://doi.org/10.1093/nar/gkae241

NIDA. 2024, September 24. Cannabis (Marijuana). Retrieved from https://nida.nih.gov/research-topics/cannabis-marijuana on 2025, January 9

Notredame, C., Higgins, D. G., & Heringa, J. (2000). T-Coffee: A novel method for fast and accurate multiple sequence alignment. Journal of molecular biology, 302(1), 205-217. https://doi.org/10.1006/jmbi.2000.4042

Nunes, L. de J., & Andrade, L. G. de. (2021). APLICABILIDADE DO CANABIDIOL NO TRATAMENTO DO TRANSTORNO DO ESPECTRO AUTISTA. *Revista Ibero-Americana de Humanidades, Ciências E Educação*, *7*(10), 853–873. https://doi.org/10.51891/rease.v7i10.2622

Pratt, A. J., & MacRae, I. J. (2009). The RNA-induced Silencing Complex: A Versatile Gene-silencing Machine. *Journal of Biological Chemistry*, *284*(27), 17897–17901. https://doi.org/10.1074/jbc.r900012200

Schoborg, J. A., Clark, L. G., Choudhury, A., Hodgman, C. E., & Jewett, M. C. (2016). Yeast knockout library allows for efficient testing of genomic mutations for cell-free protein synthesis. *Synthetic and Systems Biotechnology*, *1*(1), 2–6. https://doi.org/10.1016/j.synbio.2016.02.004

Stout, J. M., Boubakir, Z., Ambrose, S. J., Purves, R. W., & Page, J. E. (2012). The hexanoyl-CoA precursor for cannabinoid biosynthesis is formed by an acyl-activating enzyme in Cannabis sativa trichomes. *The Plant Journal*, no-no. https://doi.org/10.1111/j.1365-313x.2012.04949.x

Sun, Z., Meng, H., Li, J., Wang, J., Li, Q., Wang, Y., & Zhang, Y. (2014). Identification of Novel Knockout Targets for Improving Terpenoids Biosynthesis in Saccharomyces cerevisiae. *PLoS ONE*, *9*(11), e112615. https://doi.org/10.1371/journal.pone.0112615

UniProt Consortium. (2025). UniProt: The universal protein knowledgebase in 2025. Nucleic Acids Research, 53(D1), D609–D617. https://doi.org/10.1093/nar/gkae1010

USP-EEL-Brazil - iGEM International Genetically Engineered Machine (2023). https://2023.igem.wiki/usp-eel-brazil/index.html

Wiles, D., Shanbhag, B. K., O'Brien, M., Doblin, M. S., Bacic, A., & Beddoe, T. (2022). Heterologous production of Cannabis sativa-derived specialised metabolites of medicinal significance – Insights into engineering strategies. *Phytochemistry*, *203*, 113380. https://doi.org/10.1016/j.phytochem.2022.113380

Yang, X., Matsui, T., Kodama, T., Mori, T., Zhou, X., Taura, F., … Morita, H. (2016). Structural basis for olivetolic acid formation by a polyketide cyclase from Cannabis sativa. *FEBS Journal*, *283*(6), 1088–1106.